

# Influence of Inter- and Intraband Transitions to Electron Temperature Decay in Noble Metals After Short-Pulsed Laser Heating

**Patrick E. Hopkins**

Engineering Sciences Center,  
Sandia National Laboratories,  
P.O. Box 5800, Albuquerque, NM 87185-0346  
e-mail: pehopki@sandia.gov

*This work examines the effects of photonically induced interband excitations from the d-band to states at the Fermi energy on the electron temperature decay in noble metals. The change in the electron population in the d-band and the conduction band causes a change in electron heat capacity and electron-phonon coupling factor. In noble metals, due to the large d-band to Fermi energy separation, the contributions to electron heat capacity and electron-phonon coupling factor of intra- and interband transitions can be separated. The two temperature model describing electron-phonon heat transfer after short-pulsed laser heating is solved using the expressions for heat capacity and electron-phonon coupling factor after intra- and interband excitations, and the predicted electron temperature change of the intra- and interband excited electrons are examined. A critical fluence value is defined that represents the absorbed fluence needed to fill all available states at a given photon energy above the Fermi level. At high absorbed laser fluences and pulse energies greater than the interband transition threshold, the interband and intraband contributions to thermophysical properties differ and are shown to affect temporal electron temperature profiles. [DOI: 10.1115/1.4002295]*

*Keywords: intraband transition, interband transition, electron-phonon coupling factor, short-pulsed laser heating, electronic band structure, Fermi smearing, two temperature model*

## 1 Introduction

Electron-phonon energy transfer after short-pulsed laser heating is becoming a critical factor in many nanoscale applications. As characteristic length- and time-scales continue to decrease, the thermal resistances associated with electron-phonon energy processes are becoming comparable to typical thermal resistances associated with thermal transport in [1] or across the solid interfaces [2,3] of devices. With the increasing importance of short-pulsed heating and subsequent electron-phonon processes in fundamental research and engineering applications [4–9], the need to accurately predict the thermophysics associated with these processes is rapidly increasing.

The well known two temperature model (TTM) [10], which describes the rate of energy transfer from a hot, thermalized electron system to a cooler phonon system, has been used to predict temperature changes and deduce thermophysical properties in a wide array of studies that are driven or limited by electron-phonon energy transfer, including ablation of metal targets [6,11,12], electron-phonon heat transfer in thin films [5,13,14], effects of microstructural disorder on electron-phonon scattering [15,16], excitations in nanoparticles [17–19], and electron-interface heat transfer [20–24]. In all of these aforementioned studies, a source term from an optical excitation is considered. Experimental works studying optical excitations and electron-phonon coupling from short-pulsed lasers on noble metal targets have used incident laser fluences ranging from a few tenths to  $5000 \text{ J m}^{-2}$  [5,14,25–28].

However, this source term is only considered as a thermal excitation in heat transfer analyses. In the case of an incident optical excitation, such as that delivered by an ultrashort laser pulse, the incident photon energy will cause the electrons in the metal to undergo various inter- and intraband transitions. In the case of interband transitions, the population in the electronic bands participating in thermal processes will change, which will affect the electron heat capacity and electron-phonon coupling factor [8,29], subsequently affecting the predicted temperature change after the optical excitation [30].

In this paper, the effects of optically and thermally excited interband transitions from the d-band (below the Fermi surface) to the Fermi surface on the dynamic response of electron temperatures as predicted by the TMM are considered and compared with the effects of intraband excitations. Both thermal transitions from Fermi smearing [8,29] and optical excitations from incident photon energies [30] cause a change in the electronic density of states, which in turn affects the thermal properties and temperature changes after the excitation. Recently, Hopkins [31] derived expressions for the inter- and intraband contributions to electronic heat capacity and electron-phonon coupling factor. In this work, the TTM is solved using the expressions for heat capacity and electron-phonon coupling factor derived by Hopkins [31], and the predicted electron temperature changes of the intra- and interband excited electrons are examined for various absorbed laser fluences and wavelengths. A critical fluence value is defined that represents the absorbed fluence needed to fill all available states at a given photon energy above the Fermi level.

## 2 Background

Immediately after partial absorption of an incident laser pulse by the electrons in a solid, the energy of the absorbed photon,  $h\nu$ ,

Contributed by the Heat Transfer Division of ASME for publication in the JOURNAL OF HEAT TRANSFER. Manuscript received July 2, 2009; final manuscript received April 27, 2010; published online September 17, 2010. Assoc. Editor: Patrick E. Phelan.

where  $h$  is Planck's constant and  $\nu$  is the photon frequency, causes the electron to excite to a higher energy state. If the excited state is within the same energy band, this excitation is called an intraband transition. If the energy of the absorbed photon is greater than the energy of an allowable excitation between bands, then the excited electron will undergo an interband transition. Since Fermi smearing affects the available energy states within a few  $k_B T_e$  of the Fermi energy,  $\varepsilon_F$ , where  $k_B$  is Boltzmann's constant and  $T_e$  is the electron system temperature [16], the various intra- and interband transitions will relocate electrons to states below the Fermi energy to energies as high as the vacuum level, depending on  $h\nu$ .

The minimum photon energy required to excite an electron to undergo an interband transition to an empty state near the Fermi energy is called the interband transition threshold ( $ITT$ ) [5]. The  $ITT$  is dependent on the band structures and relative energies of the outermost filled and innermost partially filled or empty electron bands (relative to the nucleus). Therefore, the  $ITT$  is unique for any given material. For semiconductors and insulators, the  $ITT$  is the bandgap, and it represents the energy difference between the valence (outermost filled) and conduction (innermost empty) bands. Metals, however, are more complex since electron energy bands can overlap around the Fermi energy allowing these bands to be partially filled. This, in fact, is what makes metals better electrical conductors than semiconductors, and consequently why electron-phonon scattering is such a dominant form of electrical and thermal resistance in metals. In a transition metal, for example, the s-band/d-band crossing is at an energy equal to or greater than the Fermi energy. This produces several allowable low energy d-band (valence d-band) to s-band interband transitions along with intraband transitions in both the d<sub>1</sub>-band and the s-band. For example, Cr has interband Fermi transitions at 0.8 eV ( $ITT$ ), 1.0 eV, 1.4 eV, and 1.6 eV [32], W has transitions at 0.85 eV ( $ITT$ ), 1.6 eV, and 1.75 eV [32], and Ni has transitions at 0.25 eV ( $ITT$ ), 0.4 eV, and 1.3 eV [33]. This poses experimental difficulty in isolating the effects of interband transitions thermophysical properties [34]. However, noble metals have a very distinct, high energy  $ITT$  since the s-band/d-band crossing is significantly lower than the Fermi level, and therefore only the s-band is partially filled. Therefore, the lowest energy d-band to available s-band transition is very large for Cu (2.15 eV), Au (2.4 eV), and Ag (4 eV) [14], making these metals ideal candidates to examine the effects of interband transitions on the electron thermophysical.

Figure 1 shows various transitions in a generic noble metal. This schematic represents a noble metal due to the large separation of the d-band from the Fermi energy. The filled states are represented by the shaded regions and empty states as the non-shaded regions. An intraband transition is depicted as the electron being excited from the state near the Fermi energy in the s/p-band (filled circle) and filling an empty state (empty circle) in a higher energy in the same band. The various interband transitions are depicted by the processes from the d-band edge to the s/p-band. These transitions are shown for various temperatures— $T=0$ ,  $T_1$ , and  $T_2$ , where  $T_1 < T_2$ —to show the effects of Fermi smearing on the  $ITT$ .

Since the electronic heat capacity,  $C_e(T_e)$ , and the electron-phonon coupling factor,  $G(T_e)$ , are dependent on the population of the electron bands within a few  $k_B T_e$  of the Fermi surface [16], the density of states and the electronic distribution around the Fermi surface will dictate  $C_e(T_e)$  and  $G(T_e)$  [16]. In the case of intraband transitions, the population in the electron bands does not change, so  $C_e(T_e)$  and  $G(T_e)$  are governed by classical, low temperature, solid state theory. However, interband transitions increase/decrease the electron populations at various energies depending on the nature of the excitation, and therefore the density of states of the various bands below the Fermi surface must be taken into account.

The general form for the electron heat capacity is calculated by

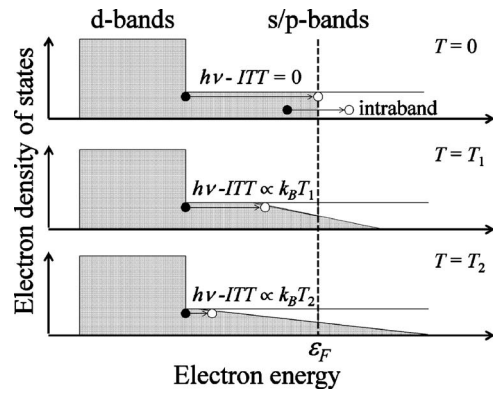


**Fig. 1** Schematic depicting intraband transition and various interband transitions in a noble metal in terms of electron density of states as a function of energy. The occupied energies are depicted by the shaded regions and the various transitions are represented as a filled circle to an unfilled circle. Whereas an intraband transition creates an electron/hole pair in the same band, an interband transition creates an electron/hole pair in different bands. The  $ITT$  is the minimum separation of the d-band edge from the Fermi energy at  $T=0$ . As the temperature is increased, photons with energies less than the  $ITT$  can excite an interband transition due to Fermi smearing which creates empty states in the s/p-bands below the Fermi energy.

$$C_e(T_e) = \int_{-\infty}^{\infty} \varepsilon D_T(\varepsilon) \frac{\partial f(\varepsilon, \mu(T_e), T_e)}{\partial T_e} d\varepsilon \quad (1)$$

where  $\varepsilon$  is the electron energy,  $D_T(\varepsilon)$  is the total density of states, and  $f$  is the Fermi-Dirac distribution function with  $\mu(T_e)$  being the chemical potential, which is a function of electron temperature. In the low temperature limit,  $\mu(T_e)$  is approximately equal to  $\varepsilon_F$ , and Eq. (1) can be expressed as  $C_e(T_e) = \gamma T_e$ , where  $\gamma$  is commonly called the Sommerfeld coefficient, which is theoretically  $62.9 \text{ J m}^{-3} \text{ K}^{-2}$  for Au [35]. The reduction of Eq. (1) to  $C_e(T_e) = \gamma T_e$  also assumes that only electrons at the Fermi energy participate in energy storage, that is,  $C_e(T_e) \propto D_C(\varepsilon_F)$  where  $D_C(\varepsilon_F)$  is the conduction band density of states.

The general form for the electron-phonon coupling factor is given by [36]

$$G(T_e) = \pi \hbar k_B \lambda \langle \omega^2 \rangle \int_{-\infty}^{\infty} \frac{(D_T(\varepsilon))^2}{D_T(\varepsilon_F)} \left( - \frac{\partial f(\varepsilon, \mu(T_e), T_e)}{\partial \varepsilon} \right) d\varepsilon \quad (2)$$

where  $\hbar$  is the reduced Planck constant,  $\lambda$  is the dimensionless electron-phonon mass enhancement parameter [37], and  $\langle \omega^2 \rangle$  is the second moment of the phonon spectrum [38]. For Au,  $\lambda \langle \omega^2 \rangle = 23 \text{ meV}^2 / \hbar^2$  [39]. In the case of only intraband transitions in the conduction band, Eq. (2) is given by

$$G(T_e) = \pi \hbar k_B \lambda \langle \omega^2 \rangle \int_{-\infty}^{\infty} \frac{(D_C(\varepsilon))^2}{D_C(\varepsilon_F)} \left( - \frac{\partial f(\varepsilon, \mu(T_e), T_e)}{\partial \varepsilon} \right) d\varepsilon \quad (3)$$

At relatively low temperatures,  $\partial f(\varepsilon, \mu(T_e), T_e) / \partial \varepsilon \approx \delta(\varepsilon - \mu(T_e)) \approx \delta(\varepsilon)$ , and Eq. (3) reduces to

$$G_0 = \pi \hbar k_B \lambda \langle \omega^2 \rangle D_C(\varepsilon_F) \quad (4)$$

which is the original expression derived by Allen [40].

In this case of interband excitations, the number density of the electrons in each band will change. The number of empty states in the conduction band for which there is sufficient photon energy to excite an electron is given by [30]

$$n_{\text{available}} = \int_{-\infty}^{\infty} D_C(\varepsilon)(1 - f(\varepsilon, \mu(T_e), T_e))(1 - H[\varepsilon - (\mu(T_e) - (\varepsilon_{ITT} - h\nu)])])d\varepsilon \quad (5)$$

where  $H[\dots]$  is the Heaviside function. Equation (5) will affect the density of states calculations. Separation of the interband and intraband contributions to electron heat capacity and electron-phonon coupling factor is discussed by Hopkins [31]. In short, the interband contribution is dependent on the band structure. In noble metals, since there is a large separation from of the d-band from the Fermi level, the contributions are additive, so  $C_{\text{total}}(T_e) = \gamma T_e + C_{\text{inter}}(T_e)$  and  $G_{\text{total}}(T_e) = G_0 + G_{\text{inter}}(T_e)$  [31].

### 3 Effects of Optical Excitations

The key to evaluating  $C_e(T_e)$  and  $G(T_e)$  lies in determining  $\mu(T_e)$ , which, when only considering intraband transitions, can be approximated by the Sommerfeld expansion [41], but when taking into account d-band excitations must be calculated by conservation of electron number density by evaluating

$$n_C + n_D = \int_{-\infty}^{\infty} (D_C(\varepsilon) + D_D(\varepsilon))f(\varepsilon, \mu(T_e), T_e)d\varepsilon \quad (6)$$

where  $n_C + n_D$  is a constant and  $\mu(T_e)$  is iterated for each temperature. For Au,  $n_C$  is  $5.9 \times 10^{28} \text{ m}^{-3}$  and  $n_D$  is  $5.9 \times 10^{29} \text{ m}^{-3}$ , which is estimated by the atomic density [35] and the number of electrons in the  $6s^1$  and  $5d^{10}$  bands, respectively [42]. The conduction band density of states is estimated by

$$D_C = 3n_{C,\text{total}}\varepsilon^{1/2}/(2\varepsilon_F^{3/2}) \quad (7)$$

where the Fermi energy of Au is 5.53 eV [35], and  $n_{C,\text{total}}$  is the total number of electrons in the conduction band after the excitation, which is given by  $n_{C,\text{total}} = n_C + n_{\text{excited}}$ . Here,  $n_{\text{excited}}$  is the number of electrons excited from the d-band to the conduction band from incident photons, which is a function of the number of photons absorbed by the material. If there are enough photons absorbed by the metal to excite all the electrons in the d-band up to available states in the conduction band, then  $n_{\text{excited}} = n_{\text{available}}$ , where  $n_{\text{available}}$  is defined by Eq. (5), and therefore  $n_{C,\text{total}} = n_C + n_{\text{available}}$ . For this condition to be true, then  $n_{\text{available}} \leq n_{\text{photons}}$ , where  $n_{\text{photons}}$  is the number of photons per unit volume in the absorbed laser pulse. The number of photons per volume can be estimated as  $n_{\text{photons}} = A/(h\nu\delta)$ , where  $A$  is the absorbed fluence and  $\delta$  is the optical penetration depth at  $h\nu$ . In the case  $n_{\text{photons}}$  is less than  $n_{\text{available}}$ , then only  $n_{\text{photons}}/n_{\text{available}}$  of the empty states in the conduction band will be filled by electrons undergoing interband transitions.

Assuming that all empty states in the conduction band below the Fermi level are filled by interband excited electrons, that is,  $n_{\text{available}} \leq n_{\text{photons}}$  and  $n_{C,\text{total}} = n_C + n_{\text{available}}$ , the number of states in the d-band after photonically induced interband transitions is given by  $n_{D,\text{total}} = n_D - n_{\text{available}}$ . The density of states of the  $5d^{10}$  band in Au can be approximated by a square function with a width of 5.28 eV [43,44] and the high energy edge of the square function 2.4 eV below the Fermi energy giving rise to the  $ITT$  energy in Au, so that

$$D_D(\varepsilon) = \frac{n_{D,\text{total}}}{5.28} (-H[\varepsilon - 3.13] + H[\varepsilon + 2.15]) \quad (8)$$

Note the calculation of temperature dependent thermophysical properties using this approximate band structure has shown close agreement with calculations of thermophysical properties using exact ab initio calculations for electronic band structure [7].

If  $n_{\text{available}} \leq n_{\text{photons}}$ , then the absorbed laser fluence must be greater than the critical fluence, which is defined as

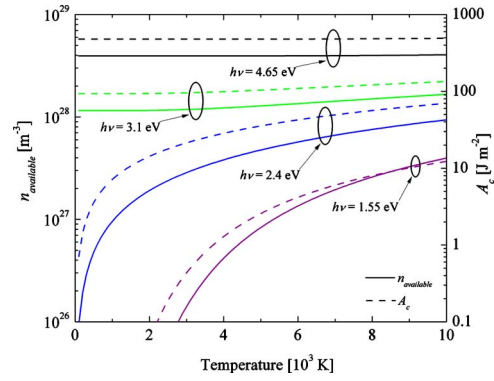


**Fig. 2** Number of available states in the conduction band,  $n_{\text{available}}$  (solid lines), as a function of temperature in Au and critical absorbed fluence required to excite enough electrons from the d-band to fill all the empty states in the conduction band,  $A_c$  (dashed lines)

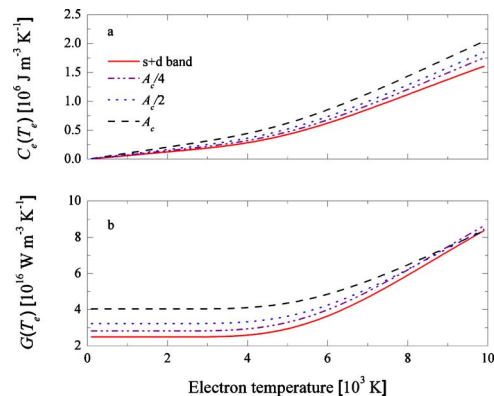
$$A_c = h\nu\delta n_{\text{available}} \quad (9)$$

Figure 2 shows  $n_{\text{available}}$  as a function of temperature for the four different photonic excitations considered, along with  $A_c$  for the different photonic excitations. The optical penetration depth,  $\delta$ , is calculated by  $\delta = \lambda/(4\pi n_2)$ , where  $n_2$  is the extinction coefficient, or the imaginary part of the complex index of refraction. The extinction coefficients in Au at 1.55, 2.4, 3.1, and 4.65 eV are 5.125, 2.120, 1.956, and 1.803, respectively [45], leading to an optical penetration depth at these energies of 12.4 nm, 19.4 nm, 16.2 nm, and 18.0 nm, respectively. The critical absorbed fluence depends on photon energy.

If the incident absorbed laser fluence is less than the critical absorbed fluence, then  $n_{\text{excited}} < n_{\text{available}}$ , and the number of electrons excited up to empty states in the conduction band from the absorbed photon energy is only  $n_{\text{excited}}/n_{\text{available}}$  of  $n_{\text{available}}$ . If the absorbed laser fluence is known, then  $n_{\text{excited}}$  can be determined by

$$n_{\text{excited}} = An_{\text{available}}/(h\nu\delta A_c) \quad (10)$$

and  $n_{C,\text{total}} = n_C + n_{\text{excited}}$  and  $n_{D,\text{total}} = n_D - n_{\text{excited}}$ . Figure 3 shows calculations for  $C_e(T_e)$  and  $G(T_e)$  for Au excited by a 4.65 eV



**Fig. 3** Predictions of (a)  $C_e(T_e)$  and (b)  $G(T_e)$  when only 50% and 25% of the available states 4.65 eV above the conduction band are filled; that is, when the absorbed fluence is only 50% or 25% of  $A_c$ . As the absorbed fluence decreases, the change in  $C_e(T_e)$  and  $G(T_e)$  from the case of no photonic excitation becomes less significant. In the limit of zero electrons excited from the d-band to empty states in the conduction band (i.e.,  $n_{\text{excited}} = 0$ ), the predictions of  $C_e(T_e)$  and  $G(T_e)$  reduce to the case of no photonic excitation (i.e., “s+d band”).

laser pulse at the critical fluence, at  $A_c/2$  and at  $A_c/4$ . The calculations for  $C_e(T_e)$  and  $G(T_e)$  for different laser pulse energies at the critical fluence are given by Hopkins [31]. For comparison, the “s+d bands” calculations, which assume no photonic excitation, are also shown in Fig. 3. As expected, a decrease in the absorbed laser fluence decreases the change in the predicted  $C_e(T_e)$  and  $G(T_e)$  from that predicted in the case of no photonic excitation.

#### 4 Intra- and Interband Transition-Dependent Two-Temperature Model

In films with thicknesses less than the thermal, or ballistic, penetration depth,  $\delta_B$ , the temperature gradient in the film is minimal, and the TTM can be expressed in a simplified form [5], given by

$$C_e(T_e) \frac{\partial T_e}{\partial t} = -G(T_e)[T_e - T_L] + \frac{0.94A}{t_p d} \exp\left[-2.77\left(\frac{t-2t_p}{t_p}\right)\right] \quad (11)$$

$$C_L \frac{\partial T_L}{\partial t} = G(T_e)[T_e - T_L] \quad (12)$$

where  $t$  is the time,  $t_p$  is the pulse width,  $d$  is the film thickness, and the subscript  $L$  refers to the lattice or phonon system. The ballistic penetration depth in Au is about 100 nm [5], so for TTM analyses assuming no thermal gradient, Au film thicknesses will be restricted to less than 100 nm. To separate the intra- and interband contributions to electron system cooling, two separate electron subsystems must be considered, where the intraband subsystem is described by

$$\gamma T_{e,\text{intra}} \frac{\partial T_{e,\text{intra}}}{\partial t} = -G_0[T_{e,\text{intra}} - T_{L,\text{intra}}] \quad (13)$$

and the cooling due to interband excitations is given by

$$C_{e,\text{inter}}(T_{e,\text{inter}}) \frac{\partial T_{e,\text{inter}}}{\partial t} = -G_{\text{inter}}(T_{e,\text{inter}})[T_{e,\text{inter}} - T_{L,\text{inter}}] \quad (14)$$

In Eqs. (13) and (14), it is assumed that the entire electron system absorbs the incident laser energy, so the initial conditions for Eqs. (13) and (14) are

$$T_{e,\text{inter}}(t=0) = T_{e,\text{intra}}(t=0) = T_{e,\text{max}} \quad (15)$$

and

$$T_{L,\text{inter}}(t=0) = T_{L,\text{intra}}(t=0) = T_L(t|_{T_{e,\text{max}}}) \quad (16)$$

where  $T_{e,\text{max}}$  is determined by Eqs. (11) and (12) and  $t|_{T_{e,\text{max}}}$  refers to the time corresponding to  $T_{e,\text{max}}$ . Figure 4 shows Eq. (13) and (14) calculations of the change in electron temperatures in a 75 nm Au film irradiated with a 500 fs laser pulse, 475 J m<sup>-2</sup> absorbed fluence and 4.65 eV photon energy (approximately the critical fluence from Fig. 2) and (b) 237 J m<sup>-2</sup> absorbed fluence and 4.65 eV photon energy (approximately half of the critical fluence from Fig. 2). Only the data after the maximum electron temperature are shown so that a delayed electron system thermalization due to the high energy pulse need not be considered [46]. Note that there is a difference in the predicted electron temperatures and rates of change (slope) of electron temperature between the intra- and interband processes. These same trends are expected for the other noble metals (Ag and Cu) since the large separation of the d-band density of states from the Fermi energy is characteristic of the noble metals [29].

The insets of Figs. 4(a) and 4(b) show the electron energy density for the inter- and intraband electron systems (the product of the heat capacity and the temperature), along with the sum of these energy densities, and the energy density obtained from the temperature predictions of Eq. (11) assuming the total values for  $C_e(T_e)$  and  $G(T_e)$  (i.e., including both intra- and interband transitions) as a function of time after the maximum electron tempera-

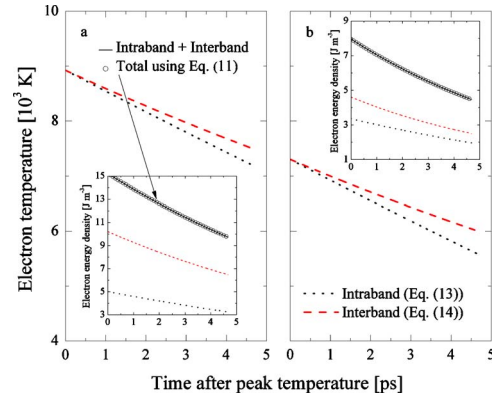


**Fig. 4** Change in temperature of electrons excited via interband (dashed lines) and intraband (dotted lines) transitions in a 75 nm Au film irradiated with a 4.65 eV, 500 fs laser pulse assuming (a) 475 J m<sup>-2</sup> absorbed fluence (approximately the critical fluence) and (b) 237 J m<sup>-2</sup> absorbed fluence (approximately 50% of the critical fluence). This temperature change was calculated with the intra- (Eq. (13)) and interband (Eq. (14)) TTMs, and assumes that the pulse has been completely absorbed and the electron system is fully thermalized. The insets show calculations of the energy densities in the inter- and intraband excited electron systems.

ture. The calculations in the inset were used to ensure that total electron energy density was conserved in the intra- and interband processes.

The traditional TTM, as described in Eqs. (11) and (12), is based on free electron theory. However, measurements using optical pulses that excite interband transitions often use this form of the TTM to determine  $G$ . As seen in Fig. 4, exciting only intraband transitions (free electrons) gives a different cooling profile than when considering only interband transitions. Since it is the cooling profile that determines  $G$  when fitting to the optical data, in the case when interband transitions are excited during these measurements, care must be taken to ensure that the thermophysical properties that account these excitations are considered.

To quantify the effects of not accounting for interband transitions after short pulse absorption, the slope of the data shown in Fig. 4 can be related to the observed electron-phonon coupling factor through the expression derived by Hohlfeld et al. [5] for a homogeneous heated film after short-pulsed laser absorption given by

$$G = -\frac{m\gamma}{1 - \frac{300}{T_{e,\text{max}}}} \quad (17)$$

where  $m$  is the observed slope of the transient temperature profile. Using Eq. (17) to calculate  $G$  from the intraband profiles in Figs. 4(a) and 4(b) gives  $2.4 \times 10^{16}$  W m<sup>-3</sup> K<sup>-1</sup>, in excellent agreement with the intraband  $G$  calculated with Eq. (4) for Au ( $2.49 \times 10^{16}$  W m<sup>-3</sup> K<sup>-1</sup>). This is expected since Eq. (17) does not take into account any subconduction band excitations; using Eq. (17) to calculate  $G$  from the interband profiles in Figs. 4(a) and 4(b) gives  $2.0 \times 10^{16}$  W m<sup>-3</sup> K<sup>-1</sup> and  $1.8 \times 10^{16}$  W m<sup>-3</sup> K<sup>-1</sup> for the high and low fluence cases, respectively. However, as seen in Fig. 3(b), the value for  $G$  when accounting for the subconduction band calculations in the temperature range 6000–9000 K ranges from  $\sim 5.0$ – $8.0 \times 10^{16}$  W m<sup>-3</sup> K<sup>-1</sup>. Therefore, if the interband transitions and d-band excitations are not accounted for when analyzing the transient electron temperature profiles, then the electron-phonon coupling factor will be under predicted of by a factor of 2.6–4.2 over the temperature range in Fig. 4. It is important to note that the differences between the inter- and intraband profiles in Fig. 4 assume that the conduction band electrons and d-band

holes excited from the laser pulse have not relaxed. After low laser fluence excitation, the electron-hole relaxation rate in metals is typically only a few tens of femtoseconds [13]. However, as the absorbed laser fluence is increased, the electron-hole relaxation time increases, and previous studies on noble metals have shown that this relaxation time can approach the electron-phonon thermalization time at laser fluences less than 1% of those of interest in this study [46–51]. Therefore, the assumption of an excited electron system that has not relaxed with the d-band holes is valid in this work and at these laser fluences, but future works should examine the low laser fluence regimes where electron-hole relaxation would be faster than electron-phonon equilibration.

## 5 Conclusions

This work examines the effects of photonically induced interband excitations from the d-band to states at the Fermi energy on the electron temperature decay in noble metals. The change in the electron population in the d-band and the conduction band causes a change in electron heat capacity and electron-phonon coupling factor, which in turn impacts the evolution of the temperature after pulse absorption and electron thermalization. In noble metals, due to the large d-band to Fermi energy separation, the contributions to electron heat capacity and electron-phonon coupling factor of intra- and interband transitions can be separated. At high absorbed laser fluences and pulse energies greater than the interband transition threshold, the interband and intraband contributions to thermophysical properties differ and are shown to affect electron temperature predictions by the two temperature model.

## Acknowledgment

The author is grateful for support from the LDRD program office through the Sandia National Laboratories Harry S. Truman Fellowship. Sandia is a multiprogram laboratory operated by Sandia Corporation, a Lockheed-Martin Co., for the United States Department of Energy's National Nuclear Security Administration under Contract No. DE-AC04-94AL85000.

## Nomenclature

$C_e$	= electron heat capacity, $\text{J m}^{-3} \text{K}^{-1}$
$D$	= electron spectral density of states per unit volume, $\text{m}^{-3} \text{eV}^{-1}$
$f$	= Fermi-Dirac distribution function
$G$	= electron-phonon coupling factor, $\text{W m}^{-3} \text{K}^{-1}$
$H$	= Heaviside function
$h$	= Planck's constant, $\text{J s}$
$\hbar$	= Planck's constant divided by $2\pi$ , $\text{J s}$
$k_B$	= Boltzmann constant, $\text{J K}^{-1}$
$m$	= slope of transient temperature change, $\text{K s}^{-1}$
$n$	= number density, $\text{m}^{-3}$
$T_e$	= electron temperature, $\text{K}$

## Greek Symbols

$\varepsilon$	= electron energy, $\text{eV}$
$\gamma$	= Sommerfeld coefficient (linear coefficient to heat capacity), $\text{J m}^{-3} \text{K}^{-2}$
$\lambda$	= electron-phonon mass enhancement parameter
$\langle \omega^2 \rangle$	= second moment of the phonon spectrum
$\mu$	= chemical potential, $\text{eV}$
$\nu$	= photon frequency, $\text{Hz}$

## Subscripts

$C$	= conduction band
$D$	= d-band
$F$	= Fermi
inter	= interband transition
intra	= intraband transition
$T$	= total

## References

- [1] Majumdar, A., Fushinobu, K., and Hijikata, K., 1995, "Effect of Gate Voltage on Hot-Electron and Hot-Phonon Interaction and Transport in a Submicrometer Transistor," *J. Appl. Phys.*, **77**, pp. 6686–6694.
- [2] Hopkins, P. E., and Norris, P. M., 2007, "Substrate Influence in Electron-Phonon Coupling Measurements in Thin Au Films," *Appl. Surf. Sci.*, **253**, pp. 6289–6294.
- [3] Majumdar, A., and Reddy, P., 2004, "Role of Electron-Phonon Coupling in Thermal Conductance of Metal-Nonmetal Interfaces," *Appl. Phys. Lett.*, **84**, pp. 4768–4770.
- [4] Hohlfeld, J., Matthias, E., Knorren, R., and Bennemann, K. H., 1997, "Nonequilibrium Magnetization Dynamics of Nickel," *Phys. Rev. Lett.*, **78**, pp. 4861–4864.
- [5] Hohlfeld, J., Wellershoff, S. S., Gudde, J., Conrad, U., Jahnke, V., and Matthias, E., 2000, "Electron and Lattice Dynamics Following Optical Excitation of Metals," *Chem. Phys.*, **251**, pp. 237–258.
- [6] Ivanov, D. S., and Zhigilei, L. V., 2003, "Combined Atomistic-Continuum Modeling of Short-Pulse Laser Melting and Disintegration of Metal Films," *Phys. Rev. B*, **68**, pp. 064114.
- [7] Lin, Z., and Zhigilei, L. V., 2006, "Thermal Excitation of d Band Electrons in Au: Implications for Laser-Induced Phase Transformations," *Proc. SPIE*, **6261**, p. 62610U.
- [8] Lin, Z., and Zhigilei, L. V., 2007, "Temperature Dependences of the Electron-Phonon Coupling, Electron Heat Capacity and Thermal Conductivity in Ni Under Femtosecond Irradiation," *Appl. Surf. Sci.*, **253**, pp. 6295–6300.
- [9] Wellershoff, S.-S., Hohlfeld, J., Gudde, J., and Matthias, E., 1999, "The Role of Electron-Phonon Coupling in Femtosecond Laser Damage of Metals," *Appl. Phys. A: Mater. Sci. Process.*, **69**, pp. S99–S107.
- [10] Anisimov, S. I., Kapeliovich, B. L., and Perel'man, T. L., 1974, "Electron Emission From Metal Surfaces Exposed to Ultrashort Laser Pulses," *Sov. Phys. JETP*, **39**, pp. 375–377.
- [11] Zhigilei, L. V., and Ivanov, D. S., 2005, "Channels of Energy Redistribution in Short-Pulse Laser Interactions With Metal Targets," *Appl. Surf. Sci.*, **248**, pp. 433–439.
- [12] Jiang, L., and Tsai, H.-L., 2005, "Improved Two-Temperature Model and Its Application in Ultrashort Laser Heating of Metal Films," *ASME J. Heat Transfer*, **127**, pp. 1167–1173.
- [13] Qiu, T. Q., and Tien, C. L., 1993, "Heat Transfer Mechanisms During Short-Pulse Laser Heating of Metals," *ASME J. Heat Transfer*, **115**, pp. 835–841.
- [14] Eesley, G. L., 1986, "Generation of Nonequilibrium Electron and Lattice Temperatures in Copper by Picosecond Laser Pulses," *Phys. Rev. B*, **33**, pp. 2144–2151.
- [15] Hostetler, J. L., Smith, A. N., Czajkowsky, D. M., and Norris, P. M., 1999, "Measurement of the Electron-Phonon Coupling Factor Dependence on Film Thickness and Grain Size in Au, Cr, and Al," *Appl. Opt.*, **38**, pp. 3614–3620.
- [16] Qiu, T. Q., and Tien, C. L., 1993, "Size Effects on Nonequilibrium Laser Heating of Metal Films," *ASME J. Heat Transfer*, **115**, pp. 842–847.
- [17] Arbouet, A., Voisin, C., Christofilos, D., Langot, P., Del Fatti, N., Vallee, F., Lerme, J., Celep, G., Cottancin, E., Gaudry, M., Pellarin, M., Broyer, M., Maillard, M., Pileni, M. P., and Treguer, M., 2003, "Electron-Phonon Scattering in Metal Clusters," *Phys. Rev. Lett.*, **90**, p. 177401.
- [18] Hartland, G. V., 2004, "Electron-Phonon Coupling and Heat Dissipation in Metal Nanoparticles," *International Journal of Nanotechnology*, **1**, pp. 307–327.
- [19] Hodak, J. H., Henglein, A., and Hartland, G. V., 2000, "Electron-Phonon Coupling Dynamics in Very Small (Between 2 and 8 nm) Diameter Au Nanoparticles," *J. Chem. Phys.*, **112**, pp. 5942–5947.
- [20] Hopkins, P. E., 2009, "Effects of Electron-Boundary Scattering on Changes in Thermoreflectance in Thin Metal Films Undergoing Intraband Transitions," *J. Appl. Phys.*, **105**, p. 093517.
- [21] Hopkins, P. E., Kassebaum, J. L., and Norris, P. M., 2009, "Effects of Electron Scattering at Metal-Nonmetal Interfaces on Electron-Phonon Equilibration in Gold Films," *J. Appl. Phys.*, **105**, p. 023710.
- [22] Hopkins, P. E., and Norris, P. M., 2009, "Contribution of Ballistic Electron Transport to Energy Transfer During Electron-Phonon Nonequilibrium in Thin Films," *ASME J. Heat Transfer*, **131**, p. 043208.
- [23] Hopkins, P. E., Norris, P. M., Stevens, R. J., Beechem, T., and Graham, S., 2008, "Influence of Interfacial Mixing on Thermal Boundary Conductance Across a Chromium/Silicon Interface," *ASME J. Heat Transfer*, **130**, p. 062402.
- [24] Norris, P. M., and Hopkins, P. E., 2009, "Examining Interfacial Diffuse Phonon Scattering Through Transient Thermoreflectance Measurements of Thermal Boundary Conductance," *ASME J. Heat Transfer*, **131**, p. 043207.
- [25] Chan, W.-L., Averback, R. S., Cahill, D. G., and Ashkenazy, Y., 2009, "Solidification Velocities in Deeply Undercooled Silver," *Phys. Rev. Lett.*, **102**, p. 095701.
- [26] Chan, W.-L., Averback, R. S., Cahill, D. G., and Lagoutchev, A., 2008, "Dynamics of Femtosecond Laser-Induced Melting of Silver," *Phys. Rev. B*, **78**, p. 214107.
- [27] Eesley, G. L., 1983, "Observation of Nonequilibrium Electron Heating in Copper," *Phys. Rev. Lett.*, **51**, pp. 2140–2143.
- [28] Smith, A. N., and Norris, P. M., 2001, "Influence of Intraband Transitions on the Electron Thermoreflectance Response of Metals," *Appl. Phys. Lett.*, **78**, pp. 1240–1242.
- [29] Lin, Z., Zhigilei, L. V., and Celli, V., 2008, "Electron-Phonon Coupling and Electron Heat Capacity of Metals Under Conditions of Strong Electron-

- Phonon Nonequilibrium," *Phys. Rev. B*, **77**, p. 075133.
- [30] Hopkins, P. E., Duda, J. C., Salaway, R. N., Smoyer, J. L., and Norris, P. M., 2008, "Effects of Intra- and Interband Transitions on Electron-Phonon Coupling and Electron Heat Capacity After Short Pulsed Laser Heating," *Nanoscale Microscale Thermophys. Eng.*, **12**, pp. 320–333.
- [31] Hopkins, P. E., 2010, "Contributions of Inter- and Intraband Excitations to Electron Heat Capacity and Electron-Phonon Coupling in Noble Metals," *ASME J. Heat Transfer*, **132**, p. 014504.
- [32] Colavita, E., Franciosi, A., Mariani, C., and Rosei, R., 1983, "Thermoreflectance Test of W, Mo and Paramagnetic Cr Band Structures," *Phys. Rev. B*, **27**, pp. 4684–4693.
- [33] Hanus, J., Feinleib, J., and Scouler, W. J., 1967, "Low-Energy Interband Transitions and Band Structure in Nickel," *Phys. Rev. Lett.*, **19**, pp. 16–20.
- [34] Hopkins, P. E., Klopff, J. M., and Norris, P. M., 2007, "Influence of Interband Transitions on Electron-Phonon Coupling Measurements in Ni Films," *Appl. Opt.*, **46**, pp. 2076–2083.
- [35] Kittel, C., 1996, *Introduction to Solid State Physics*, Wiley, New York.
- [36] Wang, X. Y., Riffe, D. M., Lee, Y.-S., and Downer, M. C., 1994, "Time-Resolved Electron-Temperature Measurement in a Highly Excited Gold Target Using Femtosecond Thermionic Emission," *Phys. Rev. B*, **50**, pp. 8016–8019.
- [37] Grimvall, G., 1981, *Selected Topics in Solid State Physics*, North-Holland, New York.
- [38] McMillan, W. L., 1968, "Transition Temperature of Strong-Coupled Superconductors," *Phys. Rev.*, **167**, pp. 331–344.
- [39] Brorson, S. D., Kazeroonian, A., Moodera, J. S., Face, D. W., Cheng, T. K., Ippen, E. P., Dresselhaus, M. S., and Dresselhaus, G., 1990, "Femtosecond Room-Temperature Measurement of the Electron-Phonon Coupling Constant  $\gamma$  in Metallic Superconductors," *Phys. Rev. Lett.*, **64**, pp. 2172–2175.
- [40] Allen, P. B., 1987, "Theory of Thermal Relaxation of Electrons in Metals," *Phys. Rev. Lett.*, **59**, pp. 1460–1463.
- [41] Pathria, R. K., 2006, *Statistical Mechanics*, Elsevier Butterworth-Heinemann, Burlington.
- [42] Gray, D. E., 1972, *American Institute of Physics Handbook*, McGraw-Hill, New York.
- [43] Harrison, W. A., 1980, *Electronic Structure and the Properties of Solids: The Physics of the Chemical Bond*, W. H. Freeman and Company, San Francisco, CA.
- [44] Heiner, E., 1988, "Nonequilibrium Thermalized Stage of Noble Metals," *Phys. Status Solidi B*, **148**, pp. 599–609.
- [45] Palik, E. D., 1985, *Handbook of Optical Constants of Solids*, Academic, Orlando, FL.
- [46] Sun, C. K., Vallee, F., Acioli, L., Ippen, E. P., and Fujimoto, J. G., 1993, "Femtosecond Investigation of Electron Thermalization in Gold," *Phys. Rev. B*, **48**, pp. 12365–12368.
- [47] Fann, W. S., Storz, R., Tom, H. W. K., and Bokor, J., 1992, "Direct Measurement of Nonequilibrium Electron-Energy Distributions in Subpicosecond Laser-Heated Gold Films," *Phys. Rev. Lett.*, **68**, pp. 2834–2837.
- [48] Fann, W. S., Storz, R., Tom, H. W. K., and Bokor, J., 1992, "Electron Thermalization in Gold," *Phys. Rev. B*, **46**, pp. 13592–13595.
- [49] Groeneveld, R. H. M., Sprik, R., and Lagendijk, A., 1992, "Effect of a Non-thermal Electron Distribution on the Electron-Phonon Energy Relaxation Process in Noble Metals," *Phys. Rev. B*, **45**, pp. 5079–5082.
- [50] Groeneveld, R. H. M., Sprik, R., and Lagendijk, A., 1995, "Femtosecond Spectroscopy of Electron-Electron and Electron-Phonon Energy Relaxation in Ag and Au," *Phys. Rev. B*, **51**, pp. 11433–11445.
- [51] Sun, C. K., Vallee, F., Acioli, L., Ippen, E. P., and Fujimoto, J. G., 1994, "Femtosecond-Tunable Measurement of Electron Thermalization in Gold," *Phys. Rev. B*, **50**, pp. 15337–15348.